This project has received funding from the European Union's Horizon 2020 research and innovation program under grant agreement No 774499

GoJelly

A gelatinous solution to plastic pollution

D5.2 **"Chemical composition of JF mucus"**	
Deliverable No.	D5.2
WP	WP5
Task	T5.2
Project partner for deliverable	NIB, SO
Authors	Katja Klun, Rasa Slizyte
Due date	28.2.2021
Delivery date	25.2.2021
Cite this document as	Klun K, Slizyte R (2021). "Chemical composition of JF mucus". "Report". GoJelly EU project. Work Package 5, T5.2, 35 pages

Table of contents

Revision history

Version	Date	Author/ Reviewer	Notes
0.1	7.2.2021	Katja Klun, Rasa Slizyte	
0.2	10.2.2021	Dror Angel	
0.3	16.2.2021	Katja Klun, Rasa Slizyte	
0.4	22.2.2021	Jamileh Javidpour	
0.5	24.2.2021	Katja Klun	

Executive summary

In order to better understand the functionality and composition of jellyfish mucus for biofilter application in microplastic entrapment within WP5, we performed various chemical and biochemical analysis. Altogether, we analyzed nine jellyfish mucus samples from six species (*Aurelia aurita sp*, *Aequorea forskalea*, *Rhizostoma pulmo, Cotylorhiza tuberculata, Periphylla peryphilla* and *Rhopilema nomadica).* Jellyfish were harvested in five different areas: Norwegian Sea, Northern Adriatic Sea, Ionian Sea, Eastern Mediterranean Sea and at the Jerusalem Aquarium. Basic chemical analysis such as protein, carbohydrate, organic content and amino acid analysis were done on unprocessed freeze dried jellyfish mucus (U-mucus). A more in-depth analysis was done on ethanol extracted (P-mucus) mucus (on all mentioned mucuses except from *A. forskalea*) by applying amino acid and monosaccharide analysis as well as structural analysis with FTIR spectroscopy, ^{13}C NMR spectroscopy and LC-MS/MS for protein analysis.

Our results confirmed that the mucus collected from medusae is a complex and highly heterogeneous biomaterial, mainly represented by mucins (large glycoproteins), proteins, carbohydrates and enzymes. Our results showed high variability (between species and intraspecies) in organic content, as well as in protein and carbohydrate content per dry weight of mucus. Protein content was higher than carbohydrate content. The high variability in organic matter indicates that the composition of unprocessed mucus can differ both between species as well as within the same species, and might be affected by different factors (e.g. trophic ecology, life history, jellyfish fitness status, environmental variables, etc.).

The eight extracted mucus samples ("P-mucus") from five jellyfish species were investigated to better characterize their high molecular weight proteins and glycoproteins. The highest molar percentage of amino acids included glutamic acid (GLU+GLN), serine (SER), glycine (GLY), threonine (THR), alanine (ALA), valine (VAL) and lysine (LYS), though these varied among P-mucus samples. This matches previously reported jellyfish mucin amino acid composition. Monosaccharide analysis indicated that carbohydrate levels were lower and included (in descending order) arabinose (Ara), glucosamine (GlcN), galactosamine (GalN) and mannose (Man).

Structural analysis conducted with ^{13}C solid state NMR spectroscopy and FTIR spectroscopy on P-mucus samples further verified that the mucus consists of proteins, glycoproteins and carbohydrates. Both spectroscopic methods applied showed a coexistence of different functional groups (aliphatic carbon, amides, anomeric C, carboxyl groups and O-alkyl C) indicating a complex structure of the mucus layer.

The analysis of peptides and proteins by LC-MS/MS indicated that *Aurelia* sp from three different locations (Slovenia, Norway and Israel) had the highest number of identified proteins, possibly because the *Aurelia sp* transcriptome has been studied and published, whereas the transcriptomes of other jellyfish species are not available. Most of the identified proteins are involved in calcium and metal ion binding, a crucial mucus function. In addition, there are proteins involved in structural functions, catalytic activity and antioxidant activity. In *Aurelia sp*, *R. pulmo, P. peryphilla* and *R. nomadica* self-protective proteins such as metalloproteinase, serine protease inhibitors and superoxide dismutase were identified.

Finally, for the purpose of a mucus biofilter development within WP5, our findings indicate that the mucus is a highly heterogeneous and complex biomaterial, which is composed of numerous proteins, glycoproteins and other metabolites, making it difficult to replicate (in nature and in the laboratory). Mucus composition depends on its physiological status (healthy/unhealthy, stressed individual…) and its interactions with environment with biotic and abiotic factors in its environment. Altogether, this probably affects mucus composition and stability, which needs to be taken into account for biofilter application.

INTRODUCTION

Many living organisms have developed defenses to protect against microbial infection, such as surface mucus layers. Recent studies have shown that the mucus, a hydrogel-like biomaterial with specific physicochemical properties has evolved in many invertebrates, such as ctenophores and cnidarians (Bakshani et al., 2018). The mucus layer serves not only as an antimicrobial agent and physical barrier, but also enables oxygen and carbon dioxide exchange, hydration and lubrication for epithelial cells (Bakshani et al., 2018). As a physical barrier, the mucus maintains distance between potentially pathogenic bacteria and epithelial cells, by means of a viscous boundary that sloughs, thereby removing bacteria that have lodged there. In addition, the mucus exerts chemical defenses in the form of lysozyme-like enzymes that digest bacterial cell walls and secretion of secondary metabolites with antimicrobial features. It is noteworthy that the mucus layer hosts a bacterial assemblage that varies as a function of species, geographic location, physiological status and and organism health (Rivera-Ortega et al, 2018).

Many jellyfish species are known to produce and release large amounts of mucus (Ames et al., 2020). The epidermis and gastrodermis of jellyfish contain mucus secreting gland cells, which produce thin mucus layers over the external surfaces of medusae (Heeger and Möller, 1987). Under stress, during reproduction, digestion, and when dying, there is an increase in the amount of mucus is released (Patwa et al., 2015) and can reach 400 mL/kg of jellyfish per hour (Liu et al. 2018). Mucus has been found to have a role in feeding, surface cleaning, and defense against predators. The surface mucus layer is a hydrogel and is mainly composed of water (95 %) and organic compounds (5 %). The main organic component of mucus are mucin glycoproteins (3 %) and other secreted compounds such as soluble proteins, peptides, lipids and nucleic acids. Mucin glycoproteins have a complex structure and are known as one of largest natural polymers ranging from 200 kDa to 200 MDa. Their large and branched structure is responsible for the gel formation and lubrication properties. Mucin glycoproteins are polymers consisting of a single protein chain, which is connected to oligosaccharide branches through serine (Ser), or threonine (Thr) residues by O-glycoside bonds. Mucins are produced in secretory cells in the form of compact concentrated granules. During mucin secretion, calcium ions are replaced with sodium ions, which is less effective in charge screening of negative charged sites in mucins, allowing the expansion of mucins in sea water. During mucin secretion and expansion, mucins adsorb water and their volume may increase 1000–3000-fold which allows the formation of a gel structure (Bakshani et al., 2018). There are variations in mucin structure due to post-translationally added oligosaccharide side chains, which are not always precisely replicated. The protein part of the mucin glycoprotein has a repeating partial sequence of amino acids in the peptide main chain (Uzawa et al., 2009). There are only few studies in the literature that have focused on the structure and composition of jellyfish mucus.

Recently, the biotechnological potential of jellyfish mucus was recognized (Patwa et al., 2015), as a biomaterial capable of capturing nanoparticles. We have developed this idea further in the GoJelly project to assess whether jellyfish mucus could serve as a biofilter for the capture and removal of nanoplastics (NP) and microplastics (MP) from wastewater treatment plants (WWTP). Considering that mucus is a complex matrix that is rich in proteins and glycoproteins, we analyzed and evaluated its chemical and biochemical composition and structure in order to better understand its function. We performed chemical analyses on unprocessed jellyfish mucus (U-mucus) and a more in-depth analysis on extracted jellyfish mucus (P-mucus). We used known methods as well as state-of-the-art analytical

tools that will give us an in-depth analysis of biochemical composition of mucus from different jellyfish species. We used: colorimetric analysis (protein, carbohydrate and lipid quantification), High Pressure Liquid Chromatography (HPLC) (amino acid and monosaccharide analysis), protein gel electrophoresis (SDS-PAGE) for protein and glycoprotein separation, ATR-FTIR spectroscopy (structure and composition), ^{13}C NMR spectroscopy (structure and composition) and LC-MS/MS spectroscopy for protein identification (structure and composition).

STUDY DESIGN

The main objective of T5.2 was to chemically and biochemically characterise mucus collected from different jellyfish species. Thus, we planned to apply various analytical methods in order to better characterize and understand mucus function. We investigated mucus from different jellyfish species from different study areas:

- Trondheimsfjorden (Norway, Norwegian Sea):
  - *Aurelia aurita*
  - *Peryphilla peryphilla*
- Gulf of Trieste (Slovenia, Northern Adriatic Sea)
  - *Aurelia aurita*
  - *Rhizostoma pulmo*
  - *Cotylorhiza tuberculata*
  - *Aequorea forskalea*
- Gulf of Taranto (Italy, Ionian Sea)
  - *Rhizostoma pulmo*
- Jerusalem Aquarium (Israel):
  - *Aurelia sp*
- Eastern Mediterranean (Israel, Haifa):
  - *Rhopilema nomadica*

The invasive comb jellyfish mucus was not studied due to difficulties in collecting jellyfish mucus. The mucus from comb jellyfish *Mnemiopsis leidyi* was also not suggested to be further processed for biofilter in Deliverable 4.1. Altogether, we investigated nine mucus samples deriving from six jellyfish species. *Aurelia sp* mucus was collected from three locations (Norway, Israel and Slovenia), *R. pulmo* mucus was collected in Italy and Slovenia, while mucus from other species (*P. peryphilla*, *C. tuberculate, A. forskalea* and *R. nomadica*), were collected only in one location each.

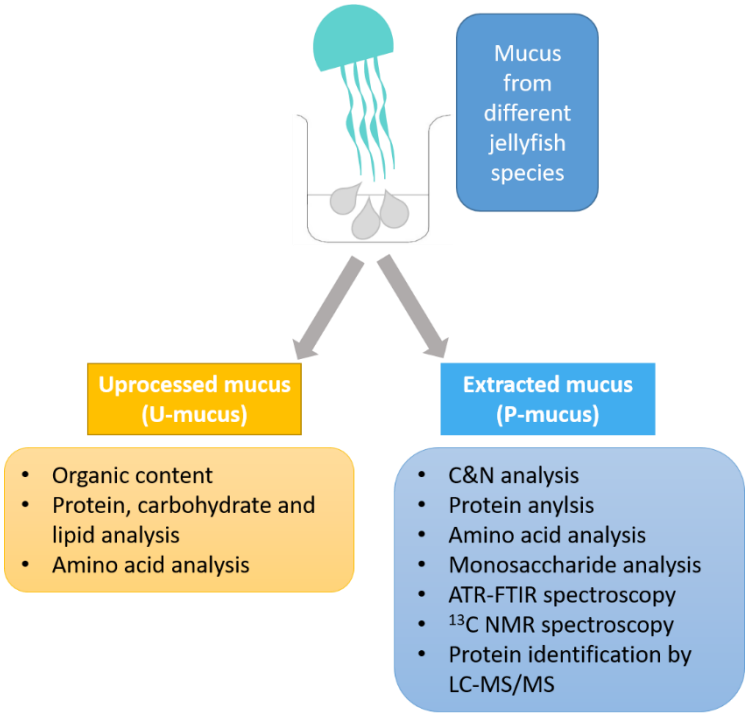

Figure 1: Schematic presentation of performed analysis on unprocessed (U-mucus) and extracted (P-mucus) mucus.

In the sections below, the mucus collection process is described, as well as sample preparation and a detail description of performed chemical and biochemical methods. The schematic presentation of analysis performed on different samples is shown in Figure 1.

JELLYFISH HARVESTING AND MUCUS COLLECTION

Jellyfish were harvested with a dip net or a trawl as described in detail in Deliverable D4.1 "Mucus collection for microplastic filter production including techniques for stabilization and preservation of jellyfish mucus" that was submitted at the end of December 2020 and as presented in Figure 2 and in Annex 2 (Table 6). All mucus was collected through the funnel (Step 1a, Figure 1), except mucus from species, *Aurelia aurita* (Slovenia) and *Cotylorhiza tuberculata* that was sampled with pipette (Step 1b, Figure 2). Mucus samples from locations outside of Slovenia were shipped frozen on dry ice to the NIB laboratories in Piran, by partners from Israel (UH), Norway (SINTEF) and Italy (CNR-ISPA).

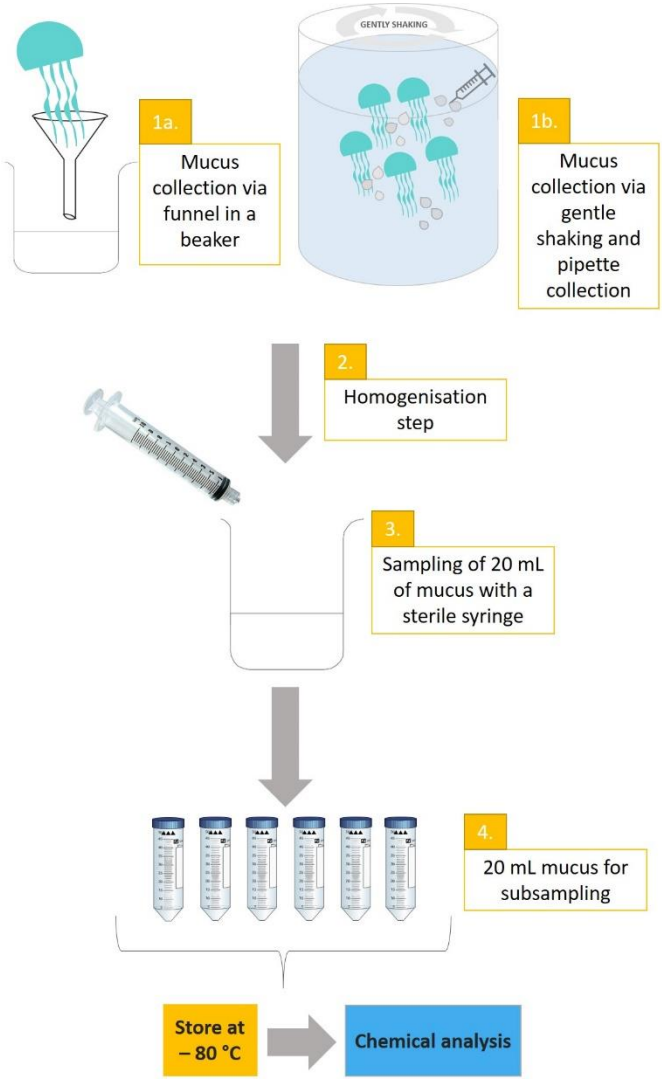

Figure 2: Jellyfish mucus collection.

SAMPLE PREPARATION

After mucus collection and storage at - 80 °C, samples were prepared for further chemical analysis. A portion of mucus was prepared for unprocessed mucus (U-mucus) analysis; the other part was processed for extraction of proteins and glycoproteins for further detailed analysis (P-Mucus).
Samples (~50 mL) for U-mucus analysis were freeze dried for 7 days, homogenized with agate mortar and pestle afterwards, and stored in the freezer for further analysis.

Samples for P-mucus (extracted mucus) analysis were prepared as described in Masuda, et al. (2007) and Patwa, et al. (2015). The mucus was collected from one individual from each species collected. Approximately 100 mL of thawed mucus was added to 150 mL (1.5 times v/v) of 0.2 % of NaCl aqueous solution at 4 °C for 24 hours. The insoluble part was removed by centrifugation at 10,000 g. After that, 96 % ethanol (ACS grade) was added (3 times of volume v/v) to obtain a gel-like precipitate. After standing overnight at 4 °C, the precipitates were separated by centrifugation, the supernatant was discarded and the pellet washed and distributed in plastic tubes with few mL of Milliq-water and stored at – 80 °C. Finally, the extracted mucus samples (P-mucus) were freeze-dried for 7 days, homogenized with agate mortar and pestle afterwards, and stored in the freezer for further analysis.

Table 1: Details of harvested jellyfish species, country, abbreviation and type of mucus analyzed.

Jellyfish species	Country	Abbreviation	U-mucus	P-mucus
Aurelia aurita	Slovenia	AA SI	✓	✓
Aurelia aurita	Norway	AA NO	✓*	✓
Aurelia sp	Israel	AA IL	-	✓
Rhizostoma pulmo	Slovenia	RP SI	✓	✓
Rhizostoma pulmo	Italy	RP IT	-	✓
Cotylorhiza tuberculate	Slovenia	CT SI	✓	✓
Peryphilla peryphilla	Norway	PP NO	✓*	✓
Rhopilema nomadica	Israel	RP IL	✓	✓
Aequorea forskalea	Slovenia	AF SI	✓	-

**P. peryphilla* (PP NO) and *A. aurita* (AA NO) U-mucus were taken only for amino acid analysis, performed at SINTEF.

ANALYTICAL METHODS

Chemical and biochemical analytical methods used are described in detail below.

ORGANIC COMPOSITION AND ELEMENTAL ANALYSIS

ASH FREE DRY MASS (AFDM) DETERMINATION

An empty ceramic cup was weighed analytically and 50 mg of each FD mucus sample was placed in the cup that was then combusted in the combustion oven at 480 °C for 4 hours. After cooling each cup was weighed again. To calculate the amount of AFDM, the mass of the cup without the sample was subtracted from the mass of the cup with the sample to get the amount of sample after combustion. Then the mass of the sample after combustion was subtracted from the mass of the sample before combustion (± 50 mg) in order to get the amount of AFDM.

ELEMENTAL ANALYSIS

Elemental composition of carbon (C) and nitrogen (N) was determined in 5 mg of dried mucus after combustion at 1150°C (Elementar, Vario Micro Cube elemental analyser) with 0.1% accuracy. The results were expressed as the relative amount of individual element per sample.

COLORIMETRIC ANALYSIS

PROTEIN

To determine the amount of protein in U-mucus and P-mucus we used QuantiPro BCA Assay Kit and followed their protocol. The principle of the bicinchoninic acid (BCA) assay relies on the formation of a Cu^{2+}-protein complex under alkaline conditions, followed by reduction of the Cu^{2+} to Cu^{1+}. The amount of reduction is proportional to protein present. BCA forms a purple-blue complex, which is detected at 562 nm, with Cu^{1+} in alkaline environments, thus providing a basis to monitor the reduction of alkaline Cu^{2+} by proteins. Bovine serum albumin (BSA) was used for standard preparation and calibration (range 0 – 30 µg / ml) (Sigma Aldrich, 2018). Protein extraction was done by adding 1.5 mL of 1x PBS (with 0.5 mM EDTA, 5 % TRITON X-100 and 1 % glycerol) to 15 mg of sample and subsequently heated at 95 °C for 5 min. After cooling (approx. 15 minutes), the samples were centrifuged (10.000 RPM) in order to remove the insoluble particles. 75 µL of supernatant was added to 75 µL of reagent prepared by QuantiPro BCA Assay instructions in a 96-well plate and incubated at 37.5 °C for 2 hours. The absorbance was measured at 562 nm. All samples were measured in triplicate.

CARBOHYDRATE

Colorimetric quantification of carbohydrates was based on the phenol-sulfuric acid reaction (Dubois et al., 1956). By adding phenol and sulphuric acid to a sample with carbohydrates, an orange-yellow colour develops, enabling us to measure the absorbance at 490 nm. D(+) Glucose was used for calibration (range 0 – 50 µg / ml). 0.5 mL of phenol and 2.5 mL of 98 % sulphuric acid was added to 50 mg of sample. After cooling, 150 µL of each sample was transferred into 96-well plate where the absorbance was measured at 490 nm with a multimode microplate reader (Spark, Tecan). All samples were measured in triplicate.

LIPID

To approximately 100 mg of freeze-dried U-mucus 4 ml of chloroform/methanol ratio 2:1 (v/v) was added. The solution was centrifuged at 4000 g for 15 min. To 500 µl of supernatant 500 µl of 98 % sulfuric acid was added. Tubes were afterwards incubated at 100 °C for 10 min and afterwards cooled on ice. To 100 µl of solution 2500 µl of phosphovanillin reagent was added and incubated at room temperature for 60 min. 150 µL of each sample was transferred into 96-well plate where the absorbance was measured at 520 nm with a multimode microplate reader (Spark, Tecan). All samples were measured in triplicate. The method is based on Folch et al. (1957) to detect polyunsaturated fatty acids.

AMINO ACID ANALYSIS

Total hydrolysable amino acid (THAA) analysis was done on U-mucus and P-mucus. SINTEF performed analysis on U-mucus, while NIB performed analysis on P-mucus as described below.

THAA NIB METHOD

To determine total hydrolysable amino acids (THAA) in P-mucus we followed method from Kaiser and Benner (2009) (with slight modifications). Approximately 10 mg of freeze dried extracted mucus was dissolved in 6 M HCl in 1.5 mL vial and 12 mM ascorbic acid was added at the end. Vials were flushed with nitrogen before sealing, heated for 20 h at 110 °C. After cooling, the subsample was dried under nitrogen stream and then diluted with 1mL milliQ water.

Analyses of THAA were done on High performance liquid chromatography system (Agilent 1260 Infinity) with fluorescence detector. Zorbax Analytical guard column (4.6 x 12.5 mm, 5 µM) and Zorbax Eclipse AAA Rapid resolution (4.6 x 150 mm, 3.5 µM) were used for L-Amino acid analysis. All glassware were carefully cleaned with 1M HCl and 3x Milli-Q and later combusted at 450 °C for 4 hours. Borate buffer (0.4 N) and OPA reagent and FMOC reagent were automatically added via the programmed autosampler to 1 ml sample for the derivatization reaction before sample was injected to the system. The separation was obtained with a flow rate of 0.8 ml min-1 with a constant temperature at 25 °C and a gradient with 4 different eluents. Calibration and peak identification was calculated from primary and secondary amino acid standard (Sigma-Aldrich). Different standard concentration were prepared from 100 nM to 10 µM. OPA reacts with primary amino acids and can be detected with fluorescence detector at excitation wavelength 340 nm and emission at 450 nm. Excitation was set at 263 nm and emission at 313 nm. Due to hydrolysis, glutamine and asparagine are oxidized and detected as glutamic acid and aspartic acid respectively, thus the results are shown as the summary of both amino acids GLU+GLN and ASP+ASN.

THAA SINTEF METHOD

The amino acid profile in freeze-dried U-mucus (unprocessed mucus) samples was analysed by a HPLC system (Agilent Infinity 1260, Agilent Technologies) coupled to an on-line post-column derivatisation module (Pinnacle PCX, Pickering laboratories, Mountain View, CA, USA), using nynhydrin (Trione) as a derivatising reagent and Na+-ion exchange column (4.6 x 110 mm, 5 µm). 18 standard amino acids, ammonia and taurin were quantified from standard curves measured with amino acid standards. Prior to the analysis, the samples were hydrolysed in 6 M HCl containing 0.4% merkaptoethanol for 24 h at 110°C (HCl hydrolysis). Glutamine and asparagine were converted to glutamic and aspartic acid, respectively. Cystein was quantified as cystin (Cys-Cys). Ammonia was separated and detected as well. The samples were filtered via micro filter, the pH was adjusted to 2.2 and the samples were further diluted with a citrate buffer (pH 2.2) for the HPLC analysis. All buffers, reagents, amino acid standards and the column were obtained from Pickering laboratories (Mountain View, CA, USA). HCl and merkaptoethanol was obtained from Sigma-Aldrich.

MONOSACCHARIDE ANALYSIS

Monosaccharide analysis were done in a commercial laboratory (Ludger Ltd) as described below. The analysis were done on P-mucus.

The monosaccharides Ara, GlcN, GalN and Man were released by incubation with 2M TFA, while monosaccharides Gal, Glc, Fuc, Rib, Xyl and Rha were released by 6M HCl for 3 hours at 100 °C. The hydrolysed samples were then labelled with a Ludger Tag™ 2AA Monosaccharide Release and Labelling Kit. 2AA labelled monosaccharides were analysed by LudgerSep-R2-HPLC following SOP-00245- Monosaccharide-HPLC-v2.0 using a LudgerSep-R2 column 4.6 x 150 mm column at 30 °C on a Waters 2795 HPLC with a fluorescence detector (λex = 360 nm, λem = 425 nm). Solvent A was BPT (made from LS-R-BPTX10) and Solvent B was acetonitrile. Gradient conditions were as follows for the 35 minute run: at a flow rate of 0.8 mL/min with 3.5% B over 7 min, followed by a gradient of 3.5-8.5% B from 7 to 25.25 min, 8.5 to 50% B over 25.25-26.25 min, 50% B from 25.25 to 26.75 min, 50-3.5% B over 26.75 - to 32.25 min at a flow rate of 1.2 mL/min, then returning to a flow of 0.8 mL/min at 35 min. The monosaccharide quantitative standards were diluted with water to produce standard curves (1 in 10 to 1 in 1000). Samples, fetuin (positive control), GPEP-A2G2S2 glycopeptide positive, and water negative controls were diluted 1 in 100 in water; 10 µL aliquots were injected onto the HPLC.

ATR-FTIR SPECTROSCOPY

Fourier-transform infrared (FT-IR) spectrometry analyses were performed on extracted samples on a Perkin-Elmer Spectrum One spectrometer with ATR accessory. Samples were filled in a micro-cup accessory. Spectra were scanned 10 times with a resolution of 4 cm^{-1} in a frequency range of 4000 to 450 cm^{-1} at room temperature.

^{13}C NMR SPECTROSCOPY

Solid-state 1D-^{13}C NMR spectra of freeze-dried extracted mucus were recorded on Agilent Technologies VNMRS 600 MHz NMR spectrometer. The experimental conditions were: number of scans 30000, pulse width 2.35 µs, spectral width 50000 Hz, acquisition time 0.025 s and pulse delay 2 s.

LC-MS/MS PROTEIN IDENTIFICATION

Protein identification was done by LC-MS/MS commercial laboratory at Institute Jožef Stefan. The jellyfish P-mucus lysate was separated on a sodium dodecyl sulfate polyacrylamide gel electrophoresis (SDS-PAGE) and each sample area was cut into six slices. Gel slices were prepared for analysis by mass spectrometer according to the standard trypsin digestion method. Slices of the gel were reduced with 10 mM DTT, alkylated with 55 mM iodoacetamide and incubated with trypsin overnight at 37 ° C. In the next step, the peptides were extracted and identified by mass spectrometry. LC-MS/MS analysis was performed using an EASY-nanoLCII HPLC unit (Proxeon) coupled to an Orbitrap LTQ Velos mass spectrometer (Thermo Scientific). Protein samples were loaded onto a C18 trapping column (Proxeon EASY-Column, 2cm, ID100 µm, 5 µm 120Å, C18-A1) and separated on a C18 PicoFrit AQUASIL analytical column (New Objective). Peptides were eluted from the column using a 90 minute linear gradient with 5-50% phase B (100% acetonitrile, 0.1% formic acid) at a constant flow rate of 300 nl/min. MS/MS spectra were obtained by HCD fragmentation of the nine most intense precursor ions in each MS cycle. Protein identification in the samples was performed using the Mascot algorithm using an NCBI nucleotide database, *Aurelia aurita* species (252634 nucleotide sequences, 11.9.2020).

RESULTS

UNPROCESSED JELLYFISH MUCUS ANALYSIS

The organic content (AFDM) results show that the lowest percentage of AFDM is in U-mucus samples of *C. tuberculata* (14.3±2.0 %) and the highest in *R. pulmo* and *A. aurita* (Table 2). Results from protein analysis of mucus from five different species show, that *R. pulmo* and *R. nomadica* mucus have the highest amount compared to the species *A. forskalea*, *C. tuberculata* and *A. aurita* that have the least amount of proteins.

Total carbohydrate contents (expressed as mg glucose/g dry weight) were lower than protein in all samples. Lowest carbohydrate values were shown in *A. forskalea* mucus. Samples from *C. tuberculata* were highly variable in terms of carbohydrate content. Highest carbohydrate concentration was observed in *R. pulmo* and *R. nomadica* (Table 2) mucus.

Lipid concentration was below the limit of detection of the method used.

Table 2: Data of U-mucus organic content (AFDM), glucose and protein concentration per dry weight.

	mg glucose / g	mg protein /g	AFDM %
AA SI	0.19±0.05	1.19±0.10	27.0±1.7
RP SI	0.42±0.18	2.54±0.51	27.0±1.4
CT SI	0.32±0.29	0.60±0.30	14.3±2.0
AF SI	0.03±0.02	0.64±0.03	26.9±0.7
RP IT	0.33±0.07	2.40±0.15	24.0±2.0
RN IL	0.55±0.12	2.75±0.25	24.3±1.3

Total amino acid analysis expressed as percentage per dry weight are presented in Table 3 below. Single amino acid content per U-mucus dry weight varied from 0.0 to 1.9 %, while the sum of single amino acid varied from 1.0 % (PP NO 7-7) to 13.1 % (RP IL). Highest amino acid content in U-mucus is shown in glutamic acid (GLU+GLN), glycine (GLY), aspartic acid (ASP+ASN) and lysine (LYS). Overall, U-mucus from PP-NO, AA-IL and RN-IL had the highest amino acid content per dry weight. Taurine (TAU), which is not an amino acid but a primary amine compound (2-aminoethanesulfonic acid), was also detected in U-mucus with highest content in RN IL U-mucus samples (1.8±0.1).

Table 3: Jellyfish U-mucus THAA percentage per dry weight of mucus collected per one individual.

% dry weight	PP NO 1	PP NO 2	PP NO 3	PP NO 4	AA NO 1	AA NO 2	AA IL	RN IL
ASP+ASN	0.2±0.0	0.1±0.0	0.1±0.0	0.5±0.0	0.3±0.0	0.3±0.0	0.3±0.0	0.8±0.0
GLU+GLN	0.4±0.0	0.2±0.0	0.3±0.0	0.7±0.0	0.5±0.0	0.6±0.0	0.5±0.0	1.9±0.1
SER	0.1±0.0	0.0±0.0	0.1±0.0	0.4±0.0	0.2±0.0	0.2±0.0	0.5±0.0	0.8±0.0
HIS	0.1±0.0	0.0±0.0	0.0±0.0	0.2±0.0	0.1±0.0	0.1±0.0	0.4±0.0	0.7±0.0
GLY	0.1±0.0	0.1±0.0	0.2±0.0	0.3±0.0	0.4±0.0	0.5±0.0	1.0±0.1	0.9±0.1
THR	0.1±0.0	0.0±0.0	0.1±0.0	0.3±0.0	0.1±0.0	0.1±0.0	0.5±0.1	0.9±0.1
ARG	0.1±0.0	0.1±0.0	0.1±0.0	0.4±0.0	0.2±0.0	0.2±0.0	0.2±0.0	0.8±0.1
ALA	0.1±0.0	0.1±0.0	0.1±0.0	0.3±0.0	0.2±0.0	0.3±0.0	0.4±0.0	1.0±0.1
TAU	0.1±0.0	0.0±0.0	0.1±0.0	0.3±0.0	0.2±0.0	0.2±0.0	0.1±0.0	1.8±0.1

TYR	0.1±0.0	0.0±0.0	0.1±0.0	0.3±0.0	0.1±0.0	0.1±0.0	0.3±0.0	0.6±0.0
VAL	0.1±0.0	0.1±0.0	0.1±0.0	0.4±0.0	0.2±0.0	0.2±0.0	0.5±0.0	1.0±0.1
PHE	0.1±0.0	0.1±0.0	0.1±0.0	0.4±0.0	0.2±0.0	0.2±0.0	0.3±0.0	0.7±0.0
ILE	0.1±0.0	0.0±0.0	0.1±0.0	0.3±0.0	0.1±0.0	0.2±0.0	0.0±0.0	0.0±0.0
LEU	0.2±0.0	0.1±0.0	0.1±0.0	0.4±0.0	0.2±0.0	0.2±0.0	0.4±0.0	1.1±0.1
LYS	0.2±0.0	0.1±0.0	0.2±0.0	0.6±0.0	0.3±0.0	0.3±0.0	0.0±0.0	0.0±0.0
PRO	0.1±0.0	0.0±0.0	0.1±0.0	0.4±0.0	0.1±0.0	0.2±0.0	-	-
CYS	0.0±0.0	0.0±0.0	0.0±0.0	0.2±0.0	0.0±0.0	0.0±0.0	-	-
HYP	-	-	-	0.0±0.0	0.0±0.0	0.0±0.0	-	-
HYL	-	-	-	-	0.0±0.0	0.0±0.0	-	-
NH4	0.1	0.0	0.0	0.1	0.1	0.1	-	-
SUM (AA)	2.5±0.0	1.0±0.0	1.9±0.0	6.5±0.0	3.6±0.0	4.1±0.0	5.4±0.2	13.1±0.8
SUM (AA+NH4)	2.6±0.0	1.0±0.0	2.0±0.0	6.6±0.0	3.6±0.0	4.2±0.0	5.4±0.2	13.1±0.8

EXTRACTED JELLYFISH MUCUS ANALYSIS

With precipitation of jellyfish mucus in ethanol, high molecular weight soluble proteins and glycoproteins were extracted from the jellyfish mucus. The extracted mucus (P-mucus) from different species was analyzed for protein, elemental C & N, amino acids and monosaccharide content (Table 4).. The lowest protein, C and N content was detected in *C. tuberculata* (CT SI), *A. aurita* (AA SI) and *R. pulmo* (RP SI) P-mucus, while the highest content was detected in *R. nomadica* P-mucus. AA SI (*A. aurita* collected in Slovenia) had much lower protein (4.0±1.3 mg/g) and carbon (0.82 %) content compared to the same species collected in Norway (23.5±1.9 mg protein/g and 7.47 % C) and Israel (31.1±0.8 mg protein/g and 9.91 % C). C/N molar ration was from 3.9 to 4.9 for all samples, which is typical for proteinaceous compounds, except the ration of CT SI was higher, 7.2.

Table 4: Protein concentration, elemental (C, N) content and C/N molar ration of P-mucus.

	Protein mg/g	% C	% N	C/N molar
CT SI	1.3±0.1	0.29	0.05	7.2
AA SI	4.0±1.3	0.82	0.20	4.9
RP SI	6.7±0.2	0.96	0.25	4.4
AA NO	23.5±1.9	7.47	2.24	3.9
PP NO	20.2±0.6	3.98	1.06	4.4
AA IL	31.1±0.8	9.91	2.74	4.2
RN IL	43.1±0.4	13.57	3.84	4.1
RP IT	30.3±1.2	7.69	1.82	4.9

Total hydrolysable amino acids (THAA)

THAA concentrations are presented in Table 5. The sum of THAA content is in accordance with protein concentration. CT SI P-mucus has the lowest THAA content and RN IL the highest content. Taurine was not detected, except in RN IL low concentrations were detected. As taurine is not an amino acid, it was also not expected to be present in P-mucus samples.

Table 5: THAA concentration (µmol per mg dry weight) in P-mucus powder.

µmol/ mg	CT SI	AA SI	AA IL	AA NO	RP SI	RP IT	PP NO	RN IL
ASP	0.8±0.0	19.5±0.9	98±4.5	67.6±3.1	4.0±0.2	126±5.8	106±4.9	702±33
GLU	3.4±0.1	33.5±1.3	153±6.1	134±5	18.6±0.7	160±6.4	93±3.7	598±24
SER	3.8±0.2	39.2±2.2	240±13	165±9	18.5±1.0	236±13	129±7.2	5.5±0.3
HIS	0.0±0.0	72.7±3.2	268±11	87.7±3.9	19.1±0.8	192±8.5	60.9±2.7	417±18
GLY	2.6±0.2	32.0±2.2	347±24	300±22	22.8±1.6	186±14	154±11	894±62
THR	3.0±0.4	56.8±7.9	293±40	167±21	18.6±2.6	285±42	123±17	797±11
ARG	0.9±0.1	13.7±1.2	124±10	99±8.5	8.1±0.7	89±7	74.3±6.4	475±41
ALA	1.5±0.1	27.6±2.0	265±18	234±18	16.6±1.2	181±12	129±9	974±70
TAU	0.0±0.0	0.0±0.0	0.0±0.0	0.0±0.0	0.6±0.0	0.0±0.0	0.0±0.0	33±2
TYR	0.0±0.0	8.0±0.4	92±4	68.2±3.4	6.4±0.3	84.4±4.2	59.0±2.9	293±14
VAL	2.0±0.1	41.6±2.5	309±18	189±13	15.8±1.0	290±19	123±7	918±53
PHE	0.7±0.1	14.0±1.0	116±8	86.6±6.3	8.5±0.6	102±7	68.1±5.0	424±30
ILE	1.3±0.1	18.2±1.0	150±8	120±6	11.2±0.6	14±7.8	93.7±5.1	577±32
LEU	1.3±0.1	23.5±1.9	215±17	179±14	14.8±1.2	18±14	121±10	845±65
LYS	1.3±0.1	38.6±2.6	266±14	201±13	18.0±1.2	188±1	138±9	1189±74
SUM	22.6±1.6	439±30	2934±205	2100±147	201±14	2432±170	1471±101	9142±641

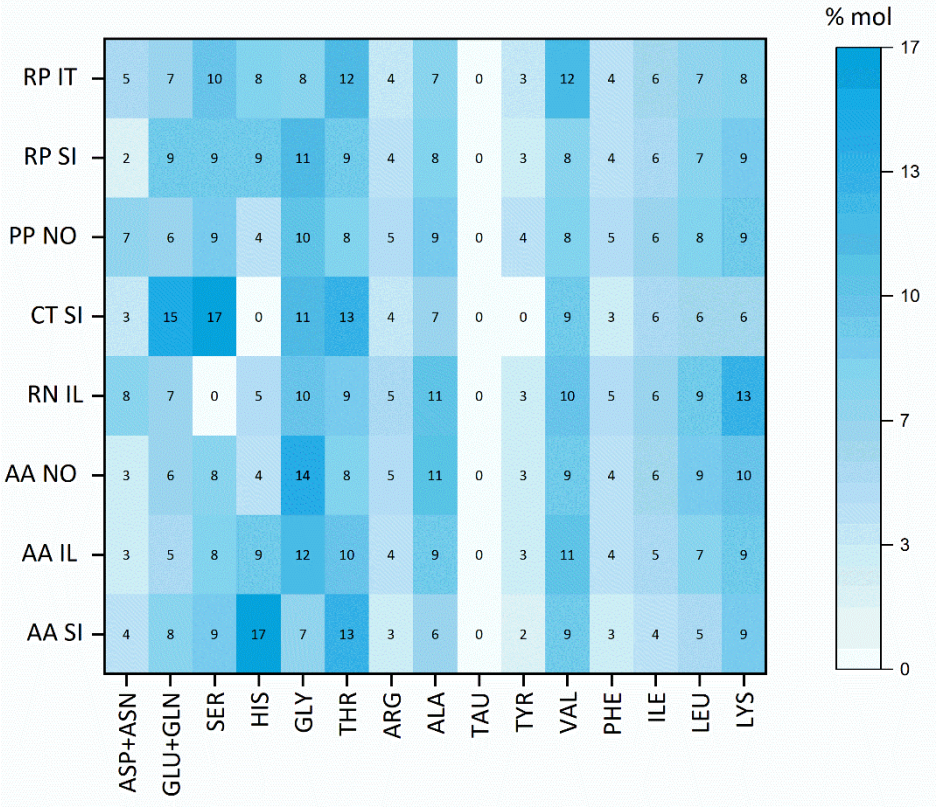

Figure 3: Amino acid (THAA) proportion in eight P-mucus samples (% mol). On the x-axis are listed amino acids.

In Figure 3, the molar percentage (% mol) of single amino acids in P-mucus samples are presented. The more intense blue in the heatmap indicates the higher molar percentage of amino acids and vice versa. The highest amino acids proportion in P-mucus were GLU (GLU+GLN), SER, GLY, THR, ALA, VAL

and LYS. CT SI P-mucus differed the most from other P-mucus samples, having a higher proportion of GLU+GLN (15 %) and SER (17 %).

Monosaccharides

Ten monosaccharides (Ara, GlcN, GalN, Man, Gal, Glc, Fuc, Rib, Xyl and Rha) were analyzed in eight P-mucus samples. The results revealed that the highest concentrations of monosaccharides were: arabinose (Ara), glucosamine (GlcN), galactosamine (GalN) and mannose (Man) (Table 6). The heatmap in Figure 4 shows that arabinose represents from 31 to 52 % of all analyzed monosaccharides.

Table 6: Monosaccharide concentration (nmol per mg dry weight) in P-mucus powder.

nmol/ mg	CT SI	AA SI	AA NO	AA IL	RP SI	RP IT	PP NO	RN IL
Ara	91.1±3.6	22.9±2.3	53.3±6.0	106.2±3.8	28.4±1.5	111.8±7.7	56.7±2.7	122.1±6.9
GlcN	25.4±1.8	6.5±0.8	11.7±1.5	23.0±2.1	20.2±2.2	90.4±8.0	19.1±2.3	28.6±2.8
GalN	33.4±1.5	7.8±0.8	19.3±2.4	35.7±2.7	14.6±0.9	71.7±5.1	26.6±2.4	32.6±2.6
Man	13.1±0.4	7.3±1.3	8.7±3.5	23.7±1.7	11.3±2.0	42.2±5.0	10.6±1.5	27.1
Gal	3.4±1.1	3.1±0.6	8.0±1.5	7.7	3.1±0.5	5.9	6.9±0.4	7.6
Glc	3.9±0.0	5.7±0.9	6.3±1.1	9.9±0.9	3.4±0.6	20.9±2.1	4.6±0.4	8.1
Fuc	0.9±0.7	0.4	0.3±0.0	0.2±0.0	0.5±0.2	0.7±0.0	0.8±0.1	0.3±0.0
Rib	-	-	47.5	-	-	-	-	-
Xyl	1.2±0.1	1.5±0.1	1.2±0.1	0.6±0.0	1.7±0.0	1.8±0.1	0.9±0.1	0.8±0.1
Rha	1.4±0.1	0.7±0.1	0.5±0.1	0.4±0.0	0.8±0.0	1.0±0.1	1.2±0.1	0.5±0.0

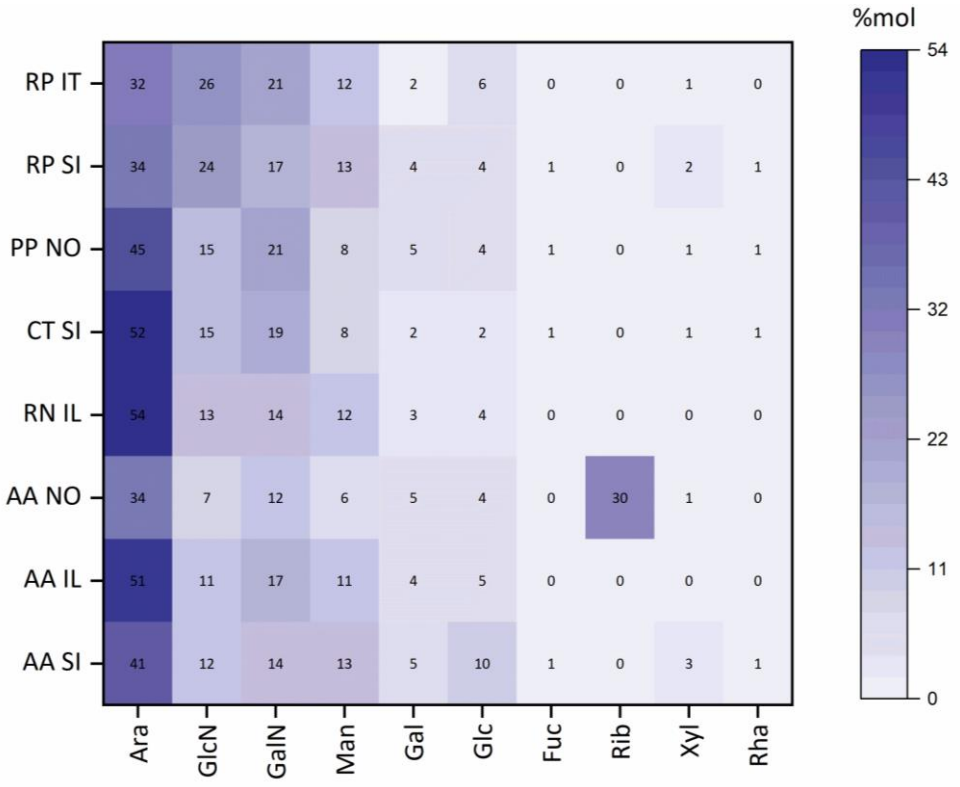

Figure 4: Monosaccharide proportion in eight P-mucus samples (% mol). On the x-axis are listed analyzed monosaccharides.

ATR-FTIR and ^{13}C solid state NMR spectroscopy

For structural analysis of jellyfish mucus (in P-mucus), we performed ATR-FTIR spectroscopy analysis and ^{13}C solid state NMR spectroscopy where functional groups were elaborated and compared between samples from different species and same species from different locations. The ATR-FTIR spectroscopy confirmed the presence of proteins and glycoproteins after assigning peaks present in the spectra. As shown in Figure 5 below, most prominent bands in all P-mucus samples are at 1500-1550 cm^{-1} (Amid II) and at 1600-1635 cm^{-1} (Amid I) that represent typical protein bands for stretching vibration of C=O (Amid I) and the N-H deformation and C-N stretching in –CO-NH (Amid II) (Guhra et al. 2020). Bands at that wavenumbers were stronger in samples of AA IL, AA NO, RP IT and RN IL. In samples of PP NO, RP SI, CT SI and AA SI the bands show much lower or zero intensity. The band at 1100 cm^{-1} is attributed to C–O–C ring vibration of polysaccharides and the band at 1028 cm^{-1} to an asymmetric stretching of C–O. The differences in intensities between P-mucus samples could be attributed due to different carbohydrate and protein content (stronger band intensity indicates higher content of specific functional group/compound).

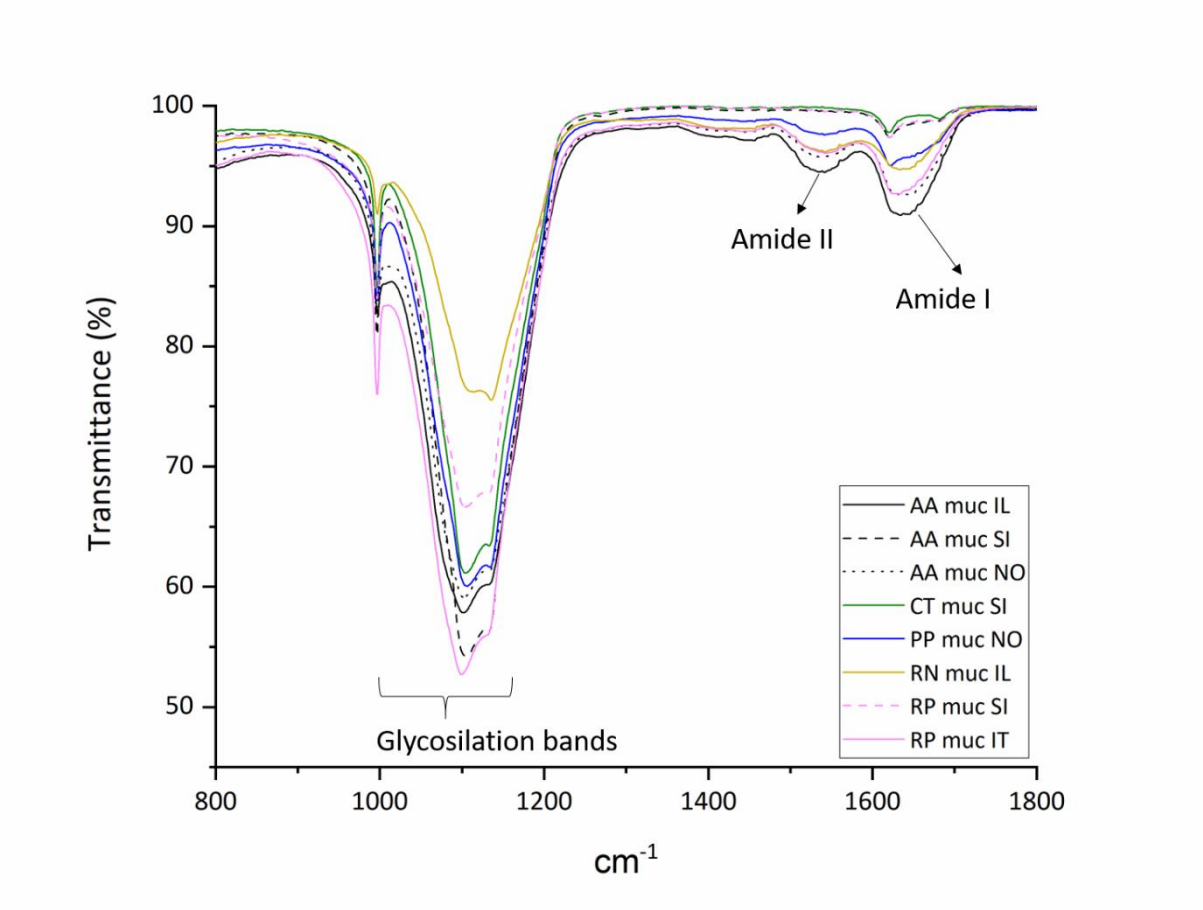

Figure 5: ATR-FTIR spectra of eight P-mucus samples.

Compared to ATR-FTIR, ^{13}C NMR can give more details on the sample composition and structure due to large chemical shift scale in ^{13}C NMR spectra, it can be divided in multiple functional groups. ATR-FTIR spectra showed typical oligosaccharide and protein bands that varied between mucus samples in band intensity due to differences in organic content and composition. The same differences were observed in ^{13}C NMR spectra as shown in Figure 6. The spectra can be divided in six chemical shifts

areas: aliphatic C (0-45 ppm), C of amino acids (45-65 ppm), O-alkyl C (65-90 ppm), anomeric C (90-110 ppm), aromatic/olefinic C (110-160 ppm) and amides/carboxyl C (160-200 ppm). The carbohydrate part is mainly seen in the regions between 65 and 110 ppm (O-alkyl C and anomeric C), while other four regions represent mostly the peptides, proteins and glycoprotein chemical shifts.

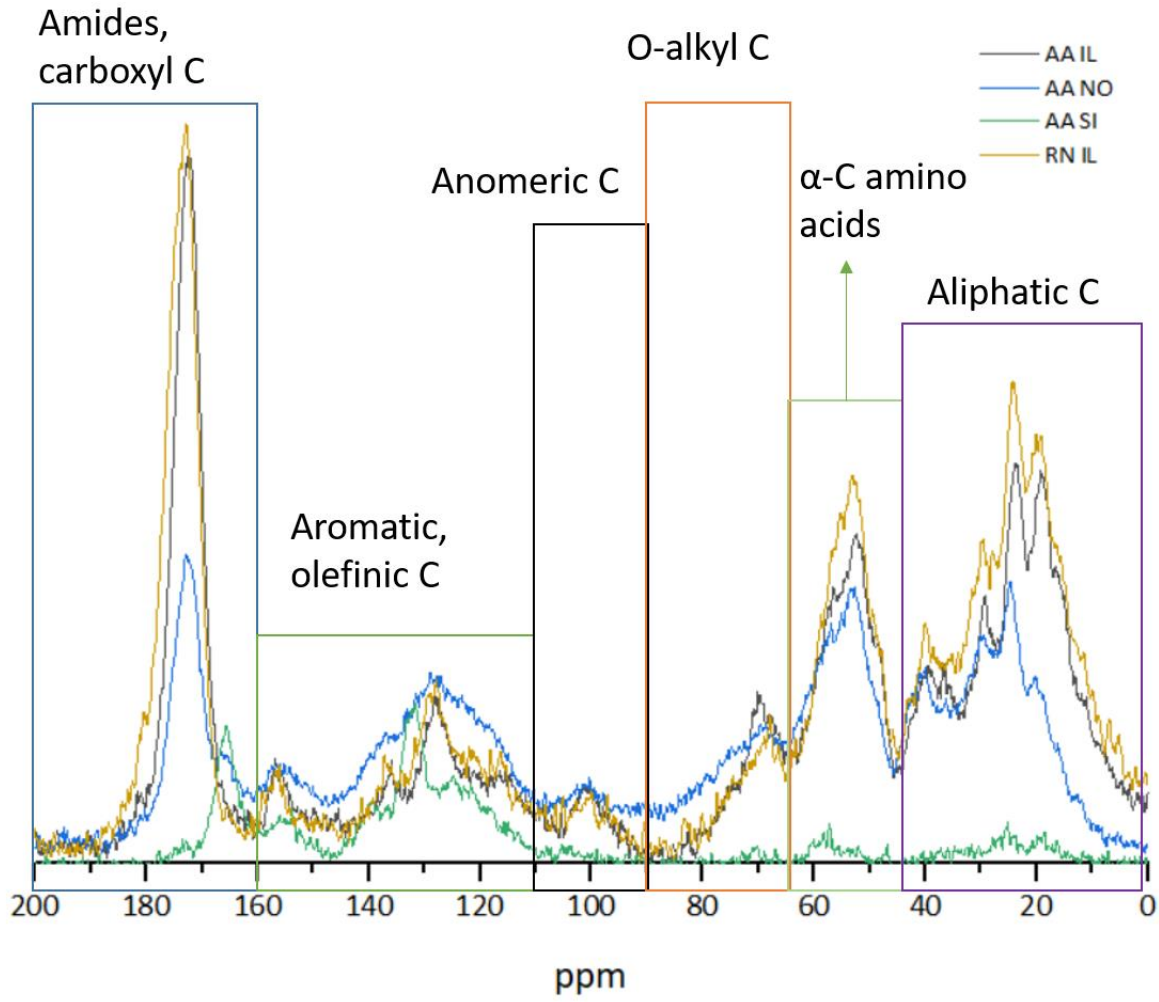

Figure 6: ^{13}C NMR solid state spectra of AA IL (gray line), AA NO (blue line), AA SI (green line) and RN IL (yellow line) P-mucus.

Mucus from *Aurelia sp.* (AA IL and AA NO) had similar band fingerprint to mucus from *R. nomadica* RN IL. Still, the AA NO sample had a little bit lower intensity compared to AA IL and RN IL in the range of amides/carboxyl C and aliphatic C. ^{13}C NMR spectra from *A. aurita* mucus collected in Slovenia showed very weak bands, which could be due to low organic content analyzed in the sample.

Protein identification

A detailed protein screening of extracted mucus samples was done by LC-MS/MS analysis. For this purpose, molecules from mucus samples were first separated using protein gel electrophoresis (SDS-PAGE), where proteins and glycoproteins are separated by their molecular weight and stained with Coomassie Brilliant Blue to detect proteins and glycoproteins (Figure 7). Strong bands are present in

AA NO, AA IL and RN IL, and the weakest in CT SI, which is in accordance with protein, carbon and amino acid concentrations.

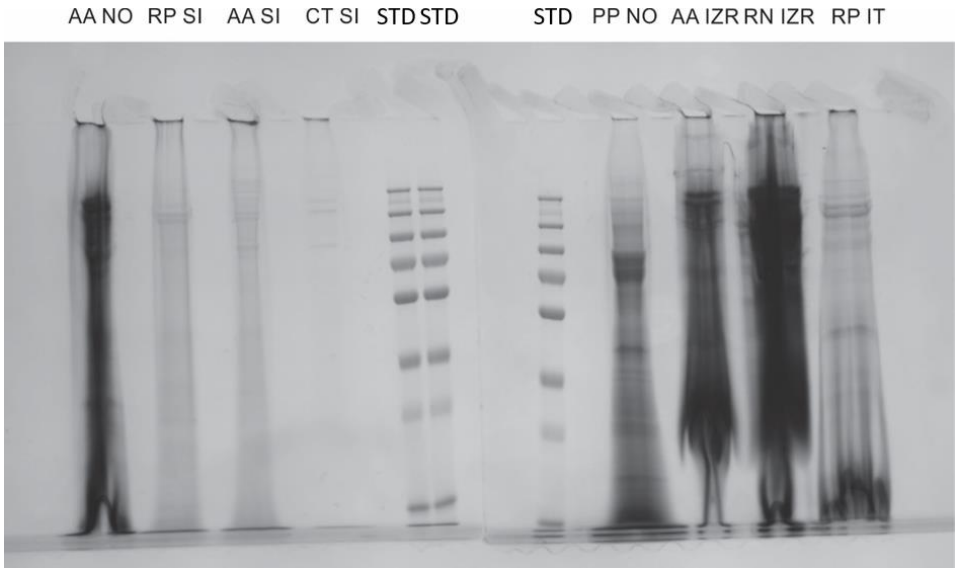

Figure 7: Scan of two SDS-PAGE gels of eight P-mucus samples (AA NO – *A. aurita* (Norway, RP SI – *R. pulmo* (Slovenia), AA SI – *A. aurita* (Slovenia), CT SI – *C. tuberculata* (Slovenia), PP NO – *P. periphylla* (Norway), AA IZR – *Aurelia sp* (Israel), RN IZR – *R. nomadica* (Israel) and RP IT – *R. pulmo* (Italy)) and protein standard (STD).

The analysis of peptide and protein with LC-MS/MS gave us an overview and function of proteins, enzymes and glycoproteins present in the mucus layer of jellyfish. The number of identified proteins against *Aurelia aurita* transcriptome are as follows: 300 in AA NO, 266 in AA IL, 215 in AA SI, 160 in RN IL, 108 in RP SI, 98 in RP IT, 36 in PP NO and 29 in CT SI. The identified proteins were mostly located in the cell's cytoskeleton and nucleus part (77-93 %), while the other portion represents the extracellular region (7-23 %). The majority of identified proteins are involved in metal ion binding, muscle contraction, DNA binding, protein binding… such as myosin, actin, histone, collagen, ubiquitin, neuricalcin, etc. Besides those proteins, other enzymes and proteins were detected that play a crucial role within surface mucus layer. The extensive table with details (accession number, protein name, main function and location) on proteins identified in each sample is presented in Table 7 in Annex 1.

The identified proteins were categorized by their function (molecular activity) according to Gene Ontology (www.uniprot.org) as presented in Figure 8. The highest number of proteins for all P-mucus samples are categorized as proteins with binding activity (Ca binding, metal ion binding, DNA binding, ATP binding…). The lowest number of proteins with binding activity was found in PP NO and CT SI P-mucus. Other proteins were categorized in structural molecular activity, catalytic activity and antioxidant activity. CT SI and PP NO P-mucus had the lowest number of proteins in all categories.

We identified also some self-protective proteins that play a crucial role within the mucus as well as proteins that may implicate mucus assembly, thus affecting mucus molecular network. Large numbers of proteins with calcium binding activity were detected and a variety of enzymes (such as protein disulfide-isomerase) that might be involved in formation and disruption of covalent bonds. Beside mentioned proteins, various serpins were present in all samples (except CT SI) that could be also involved in mucus network by binding to mucin and mucin-like glycoproteins though hydrogen bonds.

From self-protective proteins we identified metalloproteinases, serine protease inhibitors and superoxide dismutase that matched *A. aurita* transcriptome. Superoxide dismutase was not detected in CT SI and PP NO, while serine protease inhibitors were not detected only in CT SI sample. Metalloproteinase was identified only in AA IL and RP IT P-mucus sample. From mucin glycoproteins, only mucin-2 was identified, but only in AA IL, AA SI, RP IT and RP SI samples.

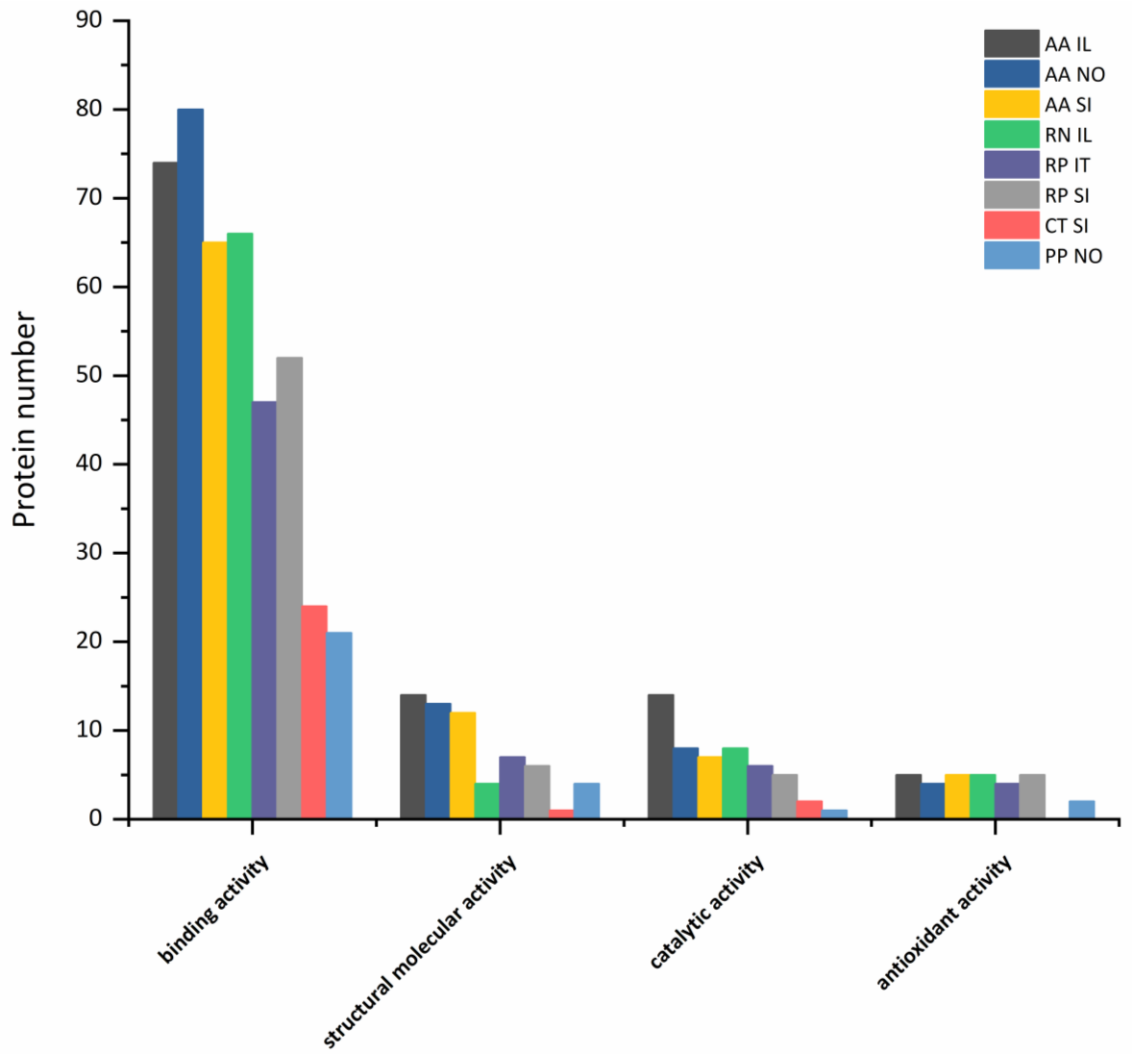

Figure 8: Comparison of protein number between eight P-mucus samples that are categorized by Gene Ontology molecular function.

DISCUSSION

The surface mucus layer is indeed a complex and highly heterogeneous biomaterial with its main functions as antibacterial defense, physical protective barrier and several physiological functions. It is known that in nature the mucus composition and its physicochemical characteristics can vary between species, environments, animal health, life stage and nutrition (Bakshani et al., 2018). There can be also variations in the mucin structure due to post-translationally added oligosaccharide side chains, which are not always precisely replicated. Mucus is mainly represented by mucins (large glycoproteins), proteins, enzymes, nucleic acids and lipids, which was also confirmed in this study.

Our results on unprocessed mucus (U-mucus) showed high variability in organic content, as well as in protein and carbohydrate content per dry weight of mucus. Variability was also observed in total hydrolysable amino acid content in U-mucus where glutamic acid (GLU+GLN), glycine (GLY), aspartic acid (ASP+ASN) and lysine (LYS) represented the highest amino acid percentage per dry weight. The sulfonic acid taurine (TAU) with various functions, one of them as a neurotransmitter, was also present in high quantities in U-mucus. Within the studied jellyfish U-mucus, proteins had the highest concentration (0.60±0.30 mg/g in CT SI to 2.75±0.25 mg/g in RN IL), followed by carbohydrates concentration (0.03±0.02 mg/g in AF SI to 0.42±0.18 mg/g), matching the pattern reported by Stabili et. al (2015). The high variability in organic content that is reflected in protein, carbohydrate and amino acid content, indicates that the composition of unprocessed mucus can differ between species as well as within species, which might be affected by different factors (individual's feeding, health, environment, stress…).

High molecular weight proteins and glycoproteins that are main constituents and play a key role in mucus's functionality were characterized in extracted mucus (P-mucus) from five jellyfish species. For this purpose, protein analysis, elemental C and N analysis, amino acid analysis, monosaccharide analysis, FTIR-spectroscopy, ^{13}C solid state NMR spectroscopy and protein identification with LC-MS/MS spectrometry were performed. The lowest protein and carbon content were in CT SI and the highest in RN IL. The same trend was observed in total hydrolysable amino acid content. The molar percentage of analyzed amino acids already indicated the presence of various proteins, glycoproteins and peptides. The highest molar percentage was shown in glutamic acid (GLU+GLN), serine (SER), glycine (GLY), threonine (THR), alanine (ALA), valine (VAL) and lysine (LYS), but varied between P-mucus samples. Mucins are known to have a repeating sequence of only a few amino acids, mostly valine, glutamic acid, serine, threonine, alanine and proline (Masuda et al. 2007; Urai et al, 2009). The fact that P-mucus samples were not further purified for only mucin characterization, we can understand that the variability in amino acid composition is due to the presence of various proteins besides the large mucins. Monosaccharide analysis showed much lower concentrations compared to amino acids. Nonetheless, the analyzed monosaccharides showed the highest concentration in arabinose (Ara), which was also reported by Masuda et al. (2007), where the novel glycoprotein from mucin family qniumucin was isolated and characterized.

With ^{13}C solid state NMR spectroscopy and FTIR spectroscopy from P-mucus samples it was shown that, the mucus is composed of chemical moieties assigned to proteins, glycoproteins and carbohydrates. Both spectroscopic methods applied showed a coexistence of different functional groups (aliphatic carbon, amides, anomeric C, carboxyl groups and O-alkyl C) indicating a complex structure of the mucus layer (Guhra et al., 2020). ^{13}C NMR spectra showed a very similar band

fingerprint in AA IL and RN IL P-mucus samples, while the AA NO specter showed lower intensity in amides/carboxyl and aliphatic region of the spectra and slightly higher in aromatic/olefinic C region, which indicates that there is a presence of less methyl groups and more lipid (unsaturated double bonds) compounds.

Based on the literature, non-mucin proteins play a key role in mucus hydrogel formation (Meldrum et al., 2018). The analysis of peptide and protein by LC-MS/MS gave us an overview of proteins, enzymes and glycoproteins present in the mucus layer, which might affect its physicochemical properties. The highest number of identified proteins were detected in samples from *A. aurita* from three different locations (Slovenia, Norway and Israel), most probably due to peptide comparison and identification with *A. aurita* transcriptome. From the investigated jellyfish species, only *A. aurita* transcriptome is known. The lowest number of identified proteins were in samples of *P. peryphilla* (PP NO) and *C. tuberculate* (CT SI). This could be due to different proteins excreted in the mucus in those species compared to *A. aurita* and/or also due to low carbon content (mostly for *C. tuberculata*). A great portion of proteins represent the extracellular matrix, while the majority is found in the inner part of the cells. The main molecular function of mucus and non-mucus proteins showed that their main activity is in binding. Most of proteins are enrolled in calcium and metal ion binding, which is a crucial part of mucus functionality. Besides that, there are proteins involved in structural molecular activity, catalytic activity and antioxidant activity. In *A. aurita*, *R. pulmo, P. peryphilla* and *R. nomadica* we identified self-protective proteins such as metalloproteinase, serine protease inhibitors (or serpins) and superoxide dismutase. The main function of metalloprotease could be to process the extracellular matrix (collagen) and to directly degrade toxic compounds or pathogen microorganisms (Liu et al, 2018). On the other hand, serpins play a key role in innate immunity and environmental stability. Superoxide dismutase are natural antioxidants that protect cellular components from reactive oxygen substances (ROS). Serpins might have an additional role in mucus network stability by binding through hydrogen bond to mucin and mucin-like glycoproteins, while protein disulfide-isomerase enzyme could affect mucus structure by both formation and disruption of covalent bonds (Meldrum et al., 2018).

Overall, the work done within T5.2 was focused on an in-depth chemical and biochemical characterization of mucus from six jellyfish species. To best of our knowledge, except the mucus of *A. aurita*, mucus from other cnidarian species explored within our study (*A. forskalea*, *R. pulmo, C. tuberculata, P. peryphilla* and *R. nomadica)* were not yet investigated. Our results confirmed the fact that surface mucus layer is a complex matrix that could be affected by many factors (environmental and physiological). The lower number of protein identified by LC-MS/MS analysis in other mucus species compared to *A. aurita* samples indicate the need of more transcriptome data of other species for a better understanding of mucus functionality. For the purpose of a mucus biofilter development within WP5, our findings indicate that the mucus is not a homogenous biomaterial but rather a highly complex matrix, where numerous proteins, glycoproteins and other metabolites were found, making it difficult to replicate. Thus, the stability of the mucus plays a crucial role in mucus application for a mucus biofilter application, which was studied within T4.1.

References

Ames, C. L., Klompen, A. M. L., Badhiwala, K., Muffett, K., Reft, A. J., Kumar, M., Janssen, J. D., Schultzhaus, J. N., Field, L. D., Muroski, M. E., Bezio, N., Robinson, J. T., Leary, D. H., Cartwright, P., Collins, A. G. & Vora, G. J. (2020) Cassiosomes are stinging-cell structures in the mucus of the upside-down jellyfish Cassiopea xamachana, *Communications Biology.* **3**, 67.

Bakshani, C. R., Morales-Garcia, A. L., Althaus, M., Wilcox, M. D., Pearson, J. P., Bythell, J. C. & Burgess, J. G. (2018) Evolutionary conservation of the antimicrobial function of mucus: a first defence against infection, *npj Biofilms and Microbiomes.* **4**, 14.

Dubois, M., Gilles, K.A., Hamilton, J.K., Rebers, P.A. & Smith, F. (1956) Colorimetric method for determination of sugars and related substances. *Analitical Chemistry*, **28**, 350–356.

Folch, J., Lees, M. & Sloane-Stanley, G.H. (1957) A simple method for the isolation and purification of total lipids from animal tissues. *J. Biol. Chem.*, **226**, 497–502

Guhra, T., Stolze, K., Schweizer, S. & Totsche, K. U. (2020) Earthworm mucus contributes to the formation of organo-mineral associations in soil, *Soil Biology and Biochemistry.* **145**, 107785.

Heeger, T. & Möller, H. (1987) Ultrastructural observations on prey capture and digestion in the scyphomedusa *Aurelia aurita*. *Marine biology*. **96**, 391–400.

Kaiser, K. & Benner, R. (2009) Biochemical composition and size distribution of organic matter at the Pacific and Atlantic time-series stations, *Marine Chemistry.* **113**, 63-77.

Masuda, A., Baba, T., Dohmae, N., Yamamura, M., Wada, H. & Ushida, K. (2007) Mucin (Qniumucin), a Glycoprotein from Jellyfish, and Determination of Its Main Chain Structure, *Journal of Natural Products.* **70**, 1089-1092.

Meldrum, O. W., Yakubov, G. E., Bonilla, M. R., Deshmukh, O., McGuckin, M. A. & Gidley, M. J. (2018) Mucin gel assembly is controlled by a collective action of non-mucin proteins, disulfide bridges, Ca2+-mediated links, and hydrogen bonding, *Scientific Reports.* **8**, 5802.

Patwa, A., Thiéry, A., Lombard, F., Lilley, M. K. S., Boisset, C., Bramard, J.-F., Bottero, J.-Y. & Barthélémy, P. (2015) Accumulation of nanoparticles in “jellyfish” mucus: a bio-inspired route to decontamination of nano-waste, *Scientific Reports.* **5**, 11387.

Rivera-Ortega, J. & Thomé, P. E. (2018) Contrasting Antibacterial Capabilities of the Surface Mucus Layer From Three Symbiotic Cnidarians, *Frontiers in Marine Science.* **5**.

Stabili, L., Schirosi, R., Parisi, M. G., Piraino, S. & Cammarata, M. (2015) The Mucus of Actinia equina (Anthozoa, Cnidaria): An Unexplored Resource for Potential Applicative Purposes, *Marine Drugs.* **13**, 5276.

Uzawa, J., Urai, M., Baba, T., Seki, H., Taniguchi, K. & Ushida, K. (2009) NMR Study on a Novel Mucin from Jellyfish in Natural Abundance, Qniumucin from Aurelia aurita, *Journal of Natural Products.* **72**, 818-823.

Annexes

ANNEX 1. SUPPLEMENTARY DATA ON PROTEIN IDENTIFICATION

Table 7: Identification of protein components in eight P-mucus samples by LC-MS/MS. The "x" sign means that the protein was detected in the sample, while "-" sign indicates that it was not present. In the table below, only known proteins with identified function are listed.

Accession number	Protein	Gene Ontology	Location	Mw	AA IL	AA NO	AA SI	CT SI	PP NO	RN IL	RP IT	RP SI
GBRG01251082.1	filamin-b isoform 4	actin cytoskeleton organization	cytoskeleton	936 kDa	x	x	x	x	x	x	x	x
GBRG01251337.1	myosin	muscle contraction	myofibril	228 kDa	x	x	x	x	x	x	x	x
GBRG01000576.1	fibrillin precursor	Ca binding	extracellular region	573 kDa	x	x	x	x	-	-	x	x
GBRG01000810.1	actin	ATP binding	nucleus, cytoskeleton	144 kDa	x	x	x	x	x	x	x	x
GBRG01000810.1	actin	ATP binding	nucleus, cytoskeleton	144 kDa	x	x	x	x	x	x	x	x
GBRG01251223.1	superfast myosin	ATP binding, actin filament binding	cytoskeleton	352 kDa	x	x	x	x	x	x	x	x
GBRG01251223.1	superfast myosin	ATP binding, actin filament binding	cytoskeleton	352 kDa	x	x	x	x	x	x	x	x
GBRG01150184.1	myosin	protein binding	myofibril	235 kDa	-	x	-	-	-	x	-	-
GBRG01134073.1	mucin-2	protective barrier of epithelia	extracellular region	438 kDa	x	-	x	-	-	-	x	x
GBRG01184077.1	heavy polypeptide	cell-cell adhesion, actin binding	cytoskeleton	582 kDa	x	x	x	x	x	x	x	x
GBRG01251499.1	neurocalcin	Ca binding		82 kDa	x	x	x	x	x	x	x	x
GBRG01251411.1	follistatin precursor	protein binding	extracellular region	171 kDa	x	x	x	x	-	-	x	x

GBRG01251883.1	fibrilar collagen	extracellular matrix structural constituent	extracellular region	426 kDa	x	x	x	x	x	x	x	x
GBRG01251247.1	col2a1a protein	metal ion binding, extracellular matrix structural constituent, collagen fibril organisation	extracellular region	429 kDa	x	x	x	-	x	x	-	x
GBRG01038818.1	histon	DNA binding	nucleus	59 kDa	x	x	x	x	x	x	x	x
GBRG01038818.1	histon	DNA binding	nucleus	59 kDa	x	x	x	x	x	x	x	x
GBRG01072253.1	histon	DNA binding	nucleus	63 kDa	-	x	x	x	x	x	x	x
GBRG01000977.1	cytochrome lyase	metal ion binding, links covalently the heme group to the apoprotein of cytochrome c.	Mitochondrion	1508 kDa	-	-	x	-	-	-	-	-
GBRG01251508.1	myosin	Ca binding, muscle contraction	cytoskeleton	102 kDa	x	x	x	x	x	x	x	x
GBRG01251508.1	myosin	Ca binding, muscle contraction	cytoskeleton	102 kDa	x	x	x	x	x	x	-	-
GBRG01088694.1	myosin	Ca binding, muscle contraction	cytoskeleton	113 kDa	x	x	x	-	x	x	x	x
GBRG01000679.1	rootletin	centrosome cycle	cytoskeleton	624 kDa	x	x	x	-	-	x	x	x
GBRG01251636.1	ubiquitin	metal ion binding	nucleus	58 kDa	x	x	x	-	x	x	x	x
GBRG01251636.1	ubiquitin	metal ion binding	nucleus	58 kDa	x	x	x	-	x	x	x	x
GBRG01251567.1	protein kinase	regulation of apoptosis, autophagy, transcription, translation and actin cytoskeleton reorganization	nucleus	210 kDa	x	x	x	-	x	x	-	-
GBRG01251567.1	protein kinase	regulation of apoptosis, autophagy, transcription, translation and actin cytoskeleton reorganization	nucleus	210 kDa	x	x	x	-	x	x	-	-
GBRG01251585.1	collagen	fibrillar forming collagen	extracellular region	391 kDa	x	x	x	-	x	x	x	x

GBRG01184516.1				291 kDa	x	-	x	-	-	x	x	x
GBRG01158507.1	myosin	protein binding	myofibril	285 kDa	x	x	x	-	-	-	-	-
GBRG01251476.1	tropomyosin	actin binding, muscle contraction	cytoskeleton	164 kDa	x	x	x	-	-	x	x	x
GBRG01251476.1	tropomyosin	actin binding, muscle contraction	cytoskeleton	164 kDa	x	x	x	-	-	x	x	x
GBRG01251230.1	disulfide isomerase	Catalyzes the rearrangement of -S-S- bonds in proteins	Endoplasmic reticulum	118 kDa	x	x	x	x	-	x	x	x
GBRG01076683.1	melanotransferrin precursor	iron binding, cellular protein metabolic process	plasma membrane	181 kDa	x	x	x	x	-	x	-	-
GBRG01076683.1	melanotransferrin precursor	iron binding, cellular protein metabolic process	plasma membrane	181 kDa	x	-	x	x	-	x	-	-
GBRG01059593.1	protein			90 kDa	x	x	x	-	-	-	-	-
GBRG01137285.1	histone	DNA binding	nucleus	182 kDa	x	x	x	x	x	x	x	x
GBRG01060649.1	tubulin beta 2c	microtubule-based process	cytoskeleton	139 kDa	x	x	x	x	-	x	x	-
GBRG01251748.1	nucleoside diphosphate kinase b	synthesis of nucleoside triphosphates other than ATP	nucleus	52 kDa	x	x	x	-	-	x	x	x
GBRG01251748.1	nucleoside diphosphate kinase b	synthesis of nucleoside triphosphates other than ATP	nucleus	52 kDa	x	x	x	-	-	x	x	x
GBRG01001808.1	histon	DNA binding, cellular protein metabolic process	nucleus	33 kDa	x	x	x	-	-	x	x	x
GBRG01000268.1	glucose-regulated protein	ATP binding	Endoplasmic reticulum	274 kDa	x	x	x	-	-	x	x	x
GBRG01251302.1	superoxide dismutase	metal ion binding; superoxide metabolic process	nucleus, mitochondrion	236 kDa	x	x	x	-	-	x	x	x
GBRG01173081.1	cytoskeleton isoform	structural constituent of cytoskeleton	cytoskeleton	409 kDa	x	x	x	-	-	x	-	-

GBRG01035046.1	histone	chromosome condensation	nucleus	71 kDa	x	x	x	-	-	x	-	x
GBRG01069184.1	calbindin	Ca binding	cytosol	126 kDa	x	x	x	-	-	-	x	x
GBRG01155023.1	fibrillin	extracellular matrix structural constituent	extracellular region	49 kDa	x	x	x	-	-	x	-	-
GBRG01251778.1	elongation factor	GTPase activity; GTP binding	nucleus	135 kDa	x	x	x	-	-	x	x	x
GBRG01251778.1	elongation factor	GTPase activity; GTP binding	nucleus	135 kDa	x	x	x	-	-	x	x	x
KC341734.1	elongation factor	GTPase activity; GTP binding	nucleus	144 kDa	x	x	x	-	-	x	x	x
GBRG01251385.1	ribosomal protein	RNA binding	nucleus and extracellular region	101 kDa	-	x	-	-	-	x	x	-
GBRG01076686.1	melanotransferrin precursor	iron binding, cellular protein metabolic process	plasma membrane	120 kDa	x	x	-	-	-	-	-	-
GBRG01251349.1	Zinc-finger protein	DNA binding	nucleolus, mitochondrion	327 kDa	x	x	-	-	-	-	-	-
GBRG01000034.1	von Willebrand factor	cellular process; binding, collagen binding	extracellular region	155 kDa	x	-	x	-	-	-	-	-
GBRG01155002.1	fibrillin	Ca binding, extracellular matrix structural constituent	extracellular region	41 kDa	x	x	x	-	-	x	x	x
GBRG01093197.1	myosin	protein binding	myofibril	253 kDa	-	x	-	-	-	-	-	-
GBRG01159370.1	Ubiquitin-like protein	enzyme binding, DNA repair	nucleus	45 kDa	x	x	x	-	x	x	x	x
GBRG01251741.1	gelsolin	calcium ion binding; actin filament severing	cytoskeleton	132 kDa	x	x	x	-	-	x	x	x
AY226077.1	elongation factor	GTPase activity; GTP binding	nucleus	62 kDa	x	x	-	-	-	-	-	-
AY226077.1	elongation factor	GTPase activity; GTP binding	nucleus	62 kDa	x	x	-	-	-	-	-	-
GBRG01251292.1	elongation factor	GTPase activity; GTP binding	nucleus	224 kDa	x	x	-	-	-	-	-	-
GBRG01000083.1	calcyphosin	Ca binding		74 kDa	x	x	x	-	-	x	-	x

GBRG01162789.1	agap007532-pa isoform 2	phagocytosis, engulfment		322 kDa	x	x	x	-	-	x	x	x
GBRG01251560.1	tropomyosin	actin binding	cytoskeleton	81 kDa	x	x	x	-	-	x	-	-
GBRG01251173.1	Protein DD3-3	May participate in O-glycosylation	membrane	139 kDa	x	x	x	-	x	-	x	x
GBRG01251173.1	Protein DD3-4	May participate in O-glycosylation	membrane	139 kDa	x	x	x	-	x	-	x	x
GBRG01163358.1	Protein DD3-5	May participate in O-glycosylation	membrane	169 kDa	x	-	-	-	-	-	x	x
GBRG01000511.1	major vault protein	ribonucleoprotein complex	nucleus	269 kDa	x	x	x	-	x	x	-	-
GBRG01000511.1	major vault protein	ribonucleoprotein complex	nucleus	269 kDa	x	x	x	-	x	x	-	-
GBRG01184511.1	massive surface protein	binding		482 kDa	x	-	x	-	-	-	-	-
GBRG01184511.1	massive surface protein	binding		482 kDa	x	-	x	-	-	-	-	-
GBRG01184512.1	massive surface protein	binding		410 kDa	x	-	x	-	-	-	-	-
GBRG01185529.1	spectrin alpha brain	Ca binding, actin binding	cytoskeleton	594 kDa	x	x	x	-	-	x	x	x
GBRG01185529.1	spectrin alpha brain	Ca binding, actin binding	cytoskeleton	594 kDa	x	x	x	-	-	x	x	x
GBRG01131244.1	type alpha partial	extracellular matrix structural constituent	extracellular region	87 kDa	-	-	x	-	-	-	x	x
GBRG01251563.1	peroxiredoxin	oxidation-reduction process	lysosome	84 kDa	x	x	x	-	-	x	-	x
GBRG01251863.1	initiation factor	mRNA-binding protein involved in translation elongation	nucleus	66 kDa	x	x	x	-	-	x	x	x
GBRG01251785.1	protein			97 kDa	x	x	x	-	-	x	x	x
GBRG01136904.1	protein			127 kDa	x	-	-	-	-	-	x	x
GBRG01251463.1	protein			117 kDa	x	x	x	-	-	-	-	x

GBRG01251519.1	glutathione s-transferase	transferase activity	cytoplasm	92 kDa	x	x	-	-	-	-	-	-
GBRG01251821.1	cytochrome c	electron transport chain	Mitochondrion	59 kDa	x	x	x	-	-	-	-	-
GBRG01155003.1	fibrillin precursor	Ca binding	extracellular region	39 kDa	x	x	-	-	-	x	x	-
GBRG01155003.1	fibrillin precursor	Ca binding	extracellular region	39 kDa	x	x	-	-	-	x	x	-
AY226057.1	alpha-tubulin	GTPase activity, microtubule-based proces	cytoskeleton	97 kDa	x	x	x	-	-	x	-	-
AY226057.1	alpha-tubulin	GTPase activity, microtubule-based proces	cytoskeleton	97 kDa	x	x	x	-	-	x	-	-
GBRG01055690.1	alpha-tubulin	GTPase activity, microtubule-based proces	cytoskeleton	84 kDa	x	-	-	-	-	x	-	-
GBRG01041048.1	protein			108 kDa	x	x	x	-	-	x	-	-
GBRG01085004.1	serpin	oxidation-reduction process, glutathione metabolic process	extracellular region	191 kDa	x	x	x	-	x	x	x	x
GBRG01085004.1	serpin	oxidation-reduction process, glutathione metabolic process	extracellular region	191 kDa	x	x	x	-	x	x	x	x
GBRG01079971.1	endoplasmin	ATP binding	Endoplasmic reticulum	267 kDa	x	x	-	x	x	x	x	x
GBRG01000027.1	14-3-3 protein zeta delta	Adapter protein implicated in the regulation of a large spectrum of both general and specialized signaling pathways	cytoplasm	191 kDa	x	x	x	-	-	x	-	-
GBRG01000027.1	14-3-3 protein zeta delta	Adapter protein implicated in the regulation of a large spectrum of both general and specialized signaling pathways	cytoplasm	191 kDa	x	x	x	-	-	x	-	-

GBRG01149467.1	14-3-3 protein epsilon	Adapter protein implicated in the regulation of a large spectrum of both general and specialized signaling pathways	cytoplasm	237 kDa	-	x	x	-	-	x	-	-
GBRG01251642.1	peroxiredoxin	Thiol-specific peroxidase that catalyzes the reduction of hydrogen peroxide and organic hydroperoxides to water and alcohols	Endoplasmic reticulum	83 kDa	x	-	x	-	-	x	x	x
GBRG01251845.1	ribosomal protein	translation; rRNA binding	cytoplasm	49 kDa	x	x	-	-	-	-	-	-
DQ467654.1 [3]	mesoglein	formation of extracellular protein fibers	extracellular region	117 kDa	x	x	x	-	-	-	-	-
DQ467654.1	mesoglein	formation of extracellular protein fibers	extracellular region	117 kDa	x	x	x	-	-	-	-	-
EF093532.1	mesoglein	formation of extracellular protein fibers	extracellular region	117 kDa	x	x	x	-	-	-	-	-
GBRG01251588.1	protein			128 kDa	x	x	x	-	-	-	-	-
GBRG01128059.1	thrombin inhibitor		extracellular region	441 kDa	x	x	x	-	-	-	-	-
GBRG01035389.1	sco-spondin	Involved in the modulation of neuronal aggregatio	extracellular region	259 kDa	x	-	x	-	-	-	-	-
GBRG01107620.1	protein			133 kDa	-	x	x	-	-	-	-	-
GBRG01000856.1	von willebrand factor d	anatomical structure development	extracellular region	372 kDa	x	-	x	-	-	-	-	-
GBRG01179481.1	hypothetical protein			657 kDa	-	x	x	-	-	x	-	-
GBRG01179481.1	hypothetical protein			657 kDa	-	x	x	-	-	x	-	-
KC341735.1	hypothetical protein			455 kDa	-	x	x	-	-	x	-	-

BY999836.1	ADP-ribosylation factor	GTP-binding protein		59 kDa	-	x	x	-	-	x	-	x
BY999836.1	ADP-ribosylation factor	GTP-binding protein		59 kDa	-	x	x	-	-	x	-	x
GBRG01082830.1	ADP-ribosylation factor	GTP-binding protein		90 kDa	-	x	x	-	-	x	-	x
GBRG01086803.1	collagen	extracellular matrix structural constituent	extracellular region	478 kDa	x	x	x	-	-	-	-	-
GBRG01178901.1	collagen	extracellular matrix structural constituent	extracellular region	224 kDa	x	x	x	-	-	-	-	-
GBRG01000120.1	protein			117 kDa	x	x	x	-	-	-	-	-
GBRG01000258.1	myosin	muscle contraction	myofibril	320 kDa	-	x	-	-	-	x	-	-
GBRG01087057.1	hemicentin	Ca binding	extracellular region	113 kDa	x	-	x	-	-	-	-	-
GBRG01132010.1	protein			27 kDa	-	-	x	-	-	-	-	-
GBRG01095718.1	Serpin peptidase inhibitor	negative regulation of endopeptidase activity	extracellular region	134 kDa	x	x	x	-	-	-	-	x
GBRG01251405.1	transcobalamin	cobalamin metabolic process	extracellular region	135 kDa	x	-	-	-	-	-	-	-
GBRG01251788.1	ribosomal protein	RNA binding	cytosol and extracellular region	52 kDa	x	x	-	-	-	x	-	-
GBRG01251267.1	isomerase	Ca binding	Endoplasmic reticulum	171 kDa	x	x	x	-	-	-	-	-
GBRG01251647.1	ribosomal protein	structural constituent of ribosome; translation	cytosol	57 kDa	x	x	-	-	-	-	x	-
GBRG01155014.1	fibrillin	Ca binding, extracellular matrix structural constituent	extracellular region	22 kDa	x	x	x	-	-	-	-	-
GBRG01251765.1	ribosomal protein	RNA binding	cytosol and extracellular region	60 kDa	x	x	-	-	-	x	-	-

GBRG01251765.1	ribosomal protein	RNA binding	cytosol and extracellular region	60 kDa	x	x	-	-	-	x	-	-
GBRG01098745.1	calmodulin	cell projection	cytoskeleton	187 kDa	x	x	x	x	-	x	-	-
GBRG01170049.1	dysferlin	protein binding	plasma membrane	626 kDa	x	x	x	-	-	x	x	x
GBRG01251605.1	ribosomal protein	RNA binding	cytosol and extracellular region	102 kDa	x	x	-	-	-	-	-	-
GBRG01251838.1	ribosomal protein	RNA binding	cytosol and extracellular region	74 kDa	x	x	-	-	-	-	-	-
GBRG01159076.1	14-3-3 protein beta alpha	enzyme binding		305 kDa	x	x	x	x	-	x	-	-
GBRG01135009.1	ubiquitin enzyme	ATP binding	cytoplasm	153 kDa	x	x	x	-	x	-	-	x
GBRG01135009.1	ubiquitin enzyme	ATP binding	cytoplasm	153 kDa	x	x	x	-	x	-	-	x
GBRG01251710.1	ribosomal protein	RNA binding	nucleus	44 kDa	-	x	-	-	-	-	x	-
GBRG01251141.1	pregnancy zone protein	endopeptidase inhibitor activity	extracellular region	418 kDa	x	x	x	-	-	-	x	x
GBRG01155025.1	fibrillin	Ca binding, extracellular matrix structural constituent	extracellular region	39 kDa	x	x	-	-	-	x	x	x
GBRG01000351.1	calreticulin	Ca binding	endoplasmic reticulum	194 kDa	-	x	-	-	-	x	-	-
GBRG01054948.1	von willebrand factor d	anatomical structure development	extracellular region	190 kDa	x	-	x	-	-	-	-	-
GBRG01166133.1	Transglutaminase	metal ion binding		239 kDa	-	x	-	-	-	x	x	-
GBRG01251348.1	adenylyl cyclase-associated protein 2	actin binding	plasma membrane	150 kDa	x	x	-	-	-	-	x	-
GBRG01000064.1	high mobility protein	DNA binding		179 kDa	x	x	x	-	-	x	-	-

GBRG01251669.1	ribosomal protein	regulation of cell cycle	cytosol and extracellular region	59 kDa	x	x	-	-	-	-	x	-
GBRG01155006.1	fibrillin	Ca binding, extracellular matrix structural constituent	extracellular region	32 kDa	x	x	-	-	-	x	x	x
GBRG01155006.1	fibrillin	Ca binding, extracellular matrix structural constituent	extracellular region	32 kDa	x	x	-	-	-	x	x	x
GBRG01126231.1	granulins-like	development, inflammation, cell proliferation and protein homeostasis	extracellular region	359 kDa	x	x	x	-	-	x	-	-
GBRG01251633.1	citrate synthase	cellular carbohydrate metabolic process	Mitochondrion	150 kDa	x	x	-	-	-	x	x	-
GBRG01251540.1	protein disulfide-isomerase	positive regulation of apoptotic process	Endoplasmic reticulum	246 kDa	x	x	x	-	-	x	x	x
GBRG01116449.1	mapmodulin	microtubule binding	Endoplasmic reticulum	126 kDa	-	x	x	-	-	x	x	x
GBRG01116449.1	mapmodulin	microtubule binding	Endoplasmic reticulum	126 kDa	-	x	x	-	-	x	x	x
GBRG01124706.1	protein			148 kDa	-	-	x	-	-	x	-	x
GBRG01124706.1	protein			148 kDa	-	-	x	-	-	x	-	x
BY999832.1	peptidylprolyl isomerase A	activation of protein kinase	extracellular region	59 kDa	x	-	-	-	-	-	-	-
GBRG01125713.1	predicted	Ca binding		303 kDa	-	-	x	-	-	-	-	x
GBRG01251486.1	s-adenosylmethionine synthase isoform	ATP binding; magnesium ion binding; response to drug	cytosol	150 kDa	x	x	x	-	-	x	x	x
GBRG01116713.1	thrombospondin type 1	Ca binding	extracellular region	170 kDa	-	-	-	x	-	x	x	x
GBRG01251862.1	ribosomal protein	RNA binding	cytosol and extracellular region	39 kDa	-	x	x	-	-	-	-	x

GBRG01115905.1	tho complex subunit	RNA binding	nucleus	151 kDa	x	x	-	-	-	x	-	-
GBRG01029853.1	protein			30 kDa	x	-	-	-	-	-	-	-
GBRG01066570.1	protein			86 kDa	x	x	x	-	-	x	x	x
GBRG01251289.1	s-adenosylhomocysteine hydrolase	adenosylhomocysteinase activity	cytoplasm	147 kDa	x	x	-	-	-	x	-	x
GBRG01251442.1	protein			135 kDa	x	-	-	-	-	-	x	-
GBRG01251442.1	protein			135 kDa	x	-	-	-	-	-	x	-
GBRG01103604.1	sushi domain-containing protein 2-like	negative regulation of cell cycle	plasma membrane	104 kDa	x	-	-	-	-	-	-	-
GBRG01074460.1	follistatin precursor	protein binding	extracellular region	146 kDa	x	-	-	-	-	-	-	-
GBRG01084096.1	serpin	protease inhibitor to modulate the host immune response	cytoplasm	300 kDa	x	-	-	-	-	-	-	-
GBRG01156227.1	collagen	extracellular matrix structural constituent	extracellular region	568 kDa	x	x	-	-	-	-	-	-
GBRG01251552.1	ribosomal protein	regulation of cell cycle	cytosol and extracellular region	95 kDa	-	x	-	-	-	-	x	-
GBRG01251291.1	astacin family metalloendopeptidase	peptidase activity, acting on L-amino acid peptides	plasma membrane	219 kDa	x	-	-	-	-	-	x	-
GBRG01251291.1	astacin family metalloendopeptidase	peptidase activity, acting on L-amino acid peptides	plasma membrane	219 kDa	x	-	-	-	-	-	x	-